

# The Surface Coat of the Mammal-dwelling Infective Trypomastigote Stage of *Trypanosoma cruzi* Is Formed by Highly Diverse Immunogenic Mucins\*

Received for publication, December 22, 2003, and in revised form, January 26, 2004  
Published, JBC Papers in Press, January 28, 2004, DOI 10.1074/jbc.M314051200

Carlos A. Buscaglia,<sup>a,b,c</sup> Vanina A. Campo,<sup>a,b,d</sup> Javier M. Di Noia,<sup>a,e</sup> Ana C. T. Torrecilhas,<sup>f,g</sup>  
Cláudia R. De Marchi,<sup>f,h</sup> Michael A. J. Ferguson,<sup>i</sup> Alberto C. C. Frasch,<sup>a,j</sup> and Igor C. Almeida<sup>f,k</sup>

From the <sup>a</sup>Instituto de Investigaciones Biotecnológicas-Instituto Tecnológico de Chascomús, Universidad Nacional de General San Martín, and the Consejo Nacional de Investigaciones Científicas y Técnicas, Avenida General Paz s/n, Predio Instituto Nacional de Tecnología Industrial, Edificio 24 (1650), San Martín, Buenos Aires, Argentina, the <sup>f</sup>Department of Parasitology, Institute of Biomedical Sciences, and the <sup>h</sup>Laboratório de Investigação Médica-Parasitologia, Instituto de Medicina Tropical, Departamento de Moléstias Infecciosas do Hospital das Clínicas, University of São Paulo, São Paulo SP 05508-000, Brazil, and the <sup>i</sup>Division of Biological Chemistry and Molecular Microbiology, Wellcome Trust Biocentre, School of Life Sciences, University of Dundee, Dundee DD1 5EH, Scotland, United Kingdom

**A thick coat of mucin-like glycoproteins covers the surface of *Trypanosoma cruzi* and plays a crucial role in parasite protection and infectivity and host immunomodulation. The appealing candidate genes coding for the mucins of the mammal-dwelling stages define a heterogeneous family termed TcMUC, which comprises up to 700 members, thus precluding a genetic approach to address the protein core identity. Here, we demonstrate by multiple approaches that the TcMUC II genes code for the majority of trypomastigote mucins. These molecules display a variable, non-repetitive, highly O-glycosylated central domain, followed by a short conserved C terminus and a glycosylphosphatidylinositol anchor. A simultaneous expression of multiple TcMUC II gene products was observed. Moreover, the C terminus of TcMUC II mucins, but not their central domain, elicited strong antibody responses in patients with Chagas' disease and *T. cruzi* infected animals. This highly diverse coat of mucins may represent a refined parasite strategy to elude the mammalian host immune system.**

*Trypanosoma cruzi* is the etiologic agent of Chagas' disease, which is of major medical and economical significance in Latin America (1). The *T. cruzi* life cycle involves distinct stages in both the mammalian host and the hematophagous insect vector (2). Within the insect, two major developmental forms can be observed: replicative epimastigotes and metacyclic trypomastigotes. The latter form brings the infection into humans when released on the skin or mucosa after the insect blood meal. Following cell invasion, metacyclic trypomastigotes differentiate into amastigotes, which, after several divisions, transform into cell-derived trypomastigotes, which are then released into the bloodstream. This stage is able to invade a wide variety of nucleated cells, thus propagating the infection.

A thick coat of glycoproteins covers the surface of all these developmental stages (3–11). The major protein components of this coat have been identified as glycosylphosphatidylinositol (GPI)<sup>1</sup>-anchored molecules enriched in Thr, Ser, and Pro residues that serve as a scaffold for the extensive addition of O-glycans (5, 8–10, 12). This particular feature enables their classification as mucin-like proteins by analogy to mammalian mucins (13). Mucins play a key role in parasite protection and infectivity and modulation of the host immune response throughout the *T. cruzi* life cycle (14–16). The mucin coat of the cell-derived trypomastigotes (tGPI-mucins) is composed of an undefined mixture of molecules ranging from 60 to 220 kDa (6, 7, 9) and sharing the stage-specific, sialic acid-containing epitope Ssp-3, critical for mammalian cell attachment/invasion (17, 18). tGPI-mucins or their GPI moieties are potent inducers of nitric oxide and pro-inflammatory cytokines by macrophages (15, 19). Major protective lytic antibodies directed against  $\alpha$ -galactosyl epitopes present in tGPI-mucins have been described in sera from chronic Chagas' disease patients (6, 7, 9, 11).

Recently, substantial information about the genetic structure and organization of mucin-like sequences in *T. cruzi* has been gained (20–26). As a result, hundreds of genes have been identified, characterized, and arranged into two separate families on the basis of sequence homology (reviewed in Refs. 14 and 27). One of these families, termed TcSMUG, is composed of

\* This work was supported in part by Fundação de Amparo à Pesquisa do Estado de São Paulo (FAPESP) Grant 98/10495-5 (Brazil) and United Nations Developmental Program/World Bank/World Health Organization-Special Program for Research and Training in Tropical Diseases Grant ID 990942 (to I. C. A.); by grants from the United Nations Developmental Program/World Bank/World Health Organization-Special Program for Research and Training in Tropical Diseases, the Agencia Nacional de Promoción Científica y Tecnológica (Argentina), and the Howard Hughes Medical Institute (to A. C. C. F.); and by a grant from the Wellcome Trust (United Kingdom) (to M. A. J. F.). The costs of publication of this article were defrayed in part by the payment of page charges. This article must therefore be hereby marked "advertisement" in accordance with 18 U.S.C. Section 1734 solely to indicate this fact.

<sup>b</sup> Both authors contributed equally to this work.

<sup>c</sup> Post-doctoral Fellow of the Consejo Nacional de Investigaciones Científicas y Técnicas. Present address: Michael Heidelberg Div. of Immunology, Dept. of Pathology, New York University School of Medicine, New York, NY 10016.

<sup>d</sup> Doctoral Fellow of the Agencia Nacional de Promoción Científica y Tecnológica (Argentina).

<sup>e</sup> Post-doctoral Fellow of the Consejo Nacional de Investigaciones Científicas y Técnicas (CONICET). Present address: Medical Research Council Lab. of Molecular Biology, Protein and Nucleic Acid Chemistry Unit, Cambridge CB2 2QH, UK.

<sup>f</sup> Doctoral Fellow of the FAPESP (Brazil).

<sup>g</sup> Researcher from CONICET.

<sup>h</sup> Research Fellow of the Conselho Nacional de Desenvolvimento Científico e Tecnológico (Brazil). To whom correspondence should be addressed: Dept. of Parasitology, Inst. of Biomedical Sciences, ICB2, University of São Paulo, Av. Prof. Lineu Prestes 1374, São Paulo SP 05508-000, Brazil. Tel.: 55-11-3091-7271; Fax: 55-11-3091-7417; E-mail: ialmeida@icb.usp.br and igorc Almeida@netscape.net.

<sup>1</sup> The abbreviations used are: GPI, glycosylphosphatidylinositol; tGPI-mucin, trypomastigote-derived glycosylphosphatidylinositol-anchored mucin; ESI-TOF-MS, electrospray time-of-flight mass spectrometry; ESI-TOF-MS/MS, electrospray time-of-flight tandem mass spectrometry; GST, glutathione S-transferase; ELISA, enzyme-linked immunosorbent assay; Hex, hexose; HexN, hexosamine.

60–70 members that were originally divided in two groups (Small and Large) according to the size of their encoded mRNAs (24). The group S gene products are most probably expressed by the insect-dwelling stages, encoding a substantial part of the 35–50-kDa mucins that cover their surface (24). The *in vivo* expression of group L has not yet been demonstrated (see Fig. 1).

Experimental evidence suggests that the second gene family, denoted as TcMUC, encodes the mucin core of the mammal-dwelling stages (20, 22, 23, 28). However, TcMUC consists of up to 700 members per haploid genome in the CL Brener clone of the parasite (22, 29), thus curtailing a genetic approach to address this issue. According to the structure of the deduced proteins, TcMUC genes were split into three major groups (22, 27). They encode 70–200-mer polypeptides that share highly homologous N- and C-terminal regions, corresponding to an endoplasmic reticulum targeting signal and a GPI anchor attachment signal, respectively. Divergences that account for their classification in different groups arise mainly in their central domains. Within this region, TcMUC I-deduced gene products contain Thr<sub>8</sub>-Lys-Pro<sub>2</sub> tandem repeats, which are suitable targets for the O-glycosylation pathway in *T. cruzi* (28, 30). Furthermore, TcMUC I products were shown to behave as functional mucins in transfected parasites and to display an antigenic hypervariable region on their mature N termini (28). On the other hand, the single gene product of the TcMUC III group (termed TSSA) has been recently identified as an antigenic dimorphic protein expressed on the mammal-derived stages, which is able to differentiate the two major *T. cruzi* phylogenetic groups (31, 32). Nevertheless, TSSA is expressed *in vivo* as a single 20-kDa product, accounting therefore for a minor subset of tGPI-mucins. Finally, the products of TcMUC II display highly variable central sequences with no Thr<sub>8</sub>-Lys-Pro<sub>2</sub> repeats, although they are rich enough in Thr, Ser, and Pro residues as to support their mucin-like denomination (see Fig. 1) (22). Hybridization analysis showed that TcMUC II genes are transcribed in variable amounts in all parasite stages (23). However, expression of TcMUC II at the protein level has never been confirmed. In this work, we demonstrate by multiple approaches that TcMUC II products are the major mucin components covering the surface of the trypomastigote stage found in the mammalian host. We also present evidence that multiple TcMUC II products are simultaneously expressed, thus suggesting a role for these molecules in *T. cruzi* immunoevasion.

#### EXPERIMENTAL PROCEDURES

**Parasites**—The CL Brener genome project reference clone and the Y strain were used throughout this study (33). Distinct *T. cruzi* stages (CL Brener clone) were obtained as described (20). Mammalian cell-derived trypomastigotes (Y strain) were obtained as described (34).

**Purification of Mammalian Cell-derived Trypomastigote Mucins**—tGPI-mucins from the Y strain were purified as described (9, 19).

**myo-Inositol and Amino Acid Analyses**—tGPI-mucins were quantified by gas chromatography-mass spectrometry with regard to their myo-inositol content (9, 35). Amino acid compositional analysis was performed according to Hendrickson and Meredith (36) as described previously (9).

**Trypsin Digestion and Purification of GPI-attached C-terminal Peptides**—tGPI-mucins (0.1–1 nmol) were incubated with 2.5–25  $\mu$ g of sequencing grade modified trypsin (Roche Diagnostics) in 10  $\mu$ l of 50 mM ammonium bicarbonate buffer (pH 8) for 18 h at 37 °C. The reaction was terminated by acidification with 0.1% formic acid. For the purification of C-terminal peptides still attached to the GPI moiety (GPI-peptides), the incubation mixture was diluted 10-fold with 100 mM ammonium acetate containing 5% 1-propanol (buffer A) and applied to a 1-ml octyl-Sepharose column (Amersham Biosciences). The column was washed with 3 ml of buffer A and submitted to stepwise elution with 1 ml of each 10, 20, 30, 40, 50, and 60% 1-propanol in buffer A. Aliquots of 10  $\mu$ l of each fraction were diluted 1:10 in 50% 1-propanol

and 10 mM ammonium acetate and analyzed by mass spectrometry as described below. tGPI-peptides were eluted at the 20% 1-propanol fraction.

**Electrospray Time-of-Flight Mass Spectrometry (ESI-TOF-MS) and Electrospray Time-of-Flight Tandem Mass Spectrometry (ESI-TOF-MS/MS) Analyses of GPI-Peptides**—GPI-peptides were analyzed by ESI-TOF-MS in a Q-tof2™ mass spectrometer (Waters Micromass Ltd., Manchester, United Kingdom). Samples (10–20  $\mu$ l) were introduced into the source by static infusion using a silica-fused nanotip. For ESI-TOF-MS analysis, the source capillary, cone, and collision energy voltages were set to 2.7 kV, 51 V, and 10 V, respectively. Scans were acquired in negative-ion mode at *m/z* 50–2000. For ESI-TOF-MS/MS analysis, the collision energy voltage was set to 45 V. All spectra were processed using MassLynx Version 3.5 software (Waters Micromass Ltd.).

**Liquid Chromatography-Mass Spectrometry Analysis of tGPI-Mucin Tryptic Peptides**—Liquid chromatography-mass spectrometry experiments were carried out using a capillary HPLC CapLC™ coupled to a Q-tof Ultima™ mass spectrometer (Waters Micromass Ltd.). A trypsin-digested tGPI-mucin sample (200 fmol, 4  $\mu$ l) was loaded onto a C<sub>18</sub> PepMap™ column (50  $\mu$ m × 300  $\mu$ m × 15 cm, LC Packings, Amsterdam, The Netherlands) and washed with 10  $\mu$ l of 0.1% formic acid at 30  $\mu$ l/min. Elution was performed at 1  $\mu$ l/min using 5% acetonitrile and 0.05% formic acid (solvent A) and 80% acetonitrile and 0.04% formic acid (solvent B) in a gradient programmed as follows: 5% solvent B, 3 min; 5–35% solvent B, 29 min; 35–80% solvent B, 3 min; 80% solvent B, 4 min; and 5% solvent B, 11 min. The eluate was introduced into the source through nanospray silica-fused tubing (360 × 75  $\mu$ m). For ESI-TOF-MS analysis, the source capillary, cone, and collision energy voltages were set to 3.15 kV, 100 V, and 10 V, respectively. Scans were acquired in positive-ion mode at *m/z* 50–2000. For ESI-TOF-MS/MS analysis, the collision energy was set to 30–40 V. All spectra were processed using MassLynx Version 3.5 software. Peptide Mass fingerprinting and ESI-TOF-MS/MS analysis were carried out using a home-made data base containing exclusively complete, mature *T. cruzi* mucin sequences (*n* = 92), most of them already deposited in the GenBank™/EBI Data Bank.<sup>2</sup> Glycopeptides and peptides were sequenced *de novo* using the Biolyx peptide sequencer function of MassLynx Version 3.5 software.

**Expression and Purification of Recombinant TcMUC II Constructs**—Six genes belonging to the TcMUC II family and obtained from the CL Brener clone were utilized: *EMUCt-4* (GenBank™/EBI accession number AY032683), *EMUC-12b9* (accession numbers AF036406 and AF036428), and *EMUCe-8* (accession number AF036420) (20) and *c2muc1*, *c2muc2*, and *c2muc3* (accession number AY298909) (26). The central domain of these genes was amplified by PCR using the following primers: *EMUCt-4*<sub>for</sub> (cgtggatccgcgatgcttaccgtcaaa) and *EMUCt-4*<sub>rev</sub> (aaggaattcaaccgaccactgacga); *c2muc1*<sub>for</sub> (cgtggatccgcttcttcaagggtgacc) and *c2muc1*<sub>rev</sub> (cggaattctgttttgcgggtgggtgtt); *c2muc3*<sub>for</sub> (cgtggatccagatcttccaatcgac) and *c2muc3*<sub>rev</sub> (cggaattcaactgtttgttctgcggatg); *EMUCe-12b9*<sub>for</sub> (cgtggatccaagtagcgaaagacagc) and *EMUCe-12b9*<sub>rev</sub> (ctgaattcagcttctcgtcagatcgt); and *EMUCe-8*<sub>for</sub> (cgtggatccagatcttccaatcgac) and *EMUCe-8*<sub>rev</sub> (acgaattcggcattttcttctactt). In addition, some genes were also amplified using the corresponding forward primer and either primer STOP (tcagccagatgggtgtacgc) or primer Thr (aagggttccactagcgtctcgt). The amplification products were cloned into pGEM™ T-Easy (Promega Corp., Madison, WI) or BamHI/EcoRI-digested and cloned into either the pGEX-2T (Amersham Biosciences) or pTrcHisA (Invitrogen) cloning vector. The ensuing recombinant proteins contained an N-terminal fusion either with glutathione S-transferase (GST) or with a stretch of six His residues. Expression and purification of both kinds of chimeric proteins were carried out as described (37).

**Immunization Procedures**—BALB/c mice (60–90 days old) were immunized intraperitoneally with 25  $\mu$ g of the corresponding GST fusion protein as described (31). Additional antisera were raised against synthetic peptides coupled through their C-terminal cysteine residue to Imject® maleimide-activated keyhole limpet hemocyanin (Pierce) following the manufacturer's guidelines.

**Enzyme-linked Immunosorbent Assay (ELISA)**—Polystyrene microplates (Maxisorp, Nunc, Roskilde, Denmark) were coated either with 100 ng of recombinant proteins or with 200 ng of bovine serum albumin-coupled peptides in phosphate-buffered saline and processed as described (31).

**Serum Survey**—Sera from untreated chronic Chagas' disease patients were either acquired from the Instituto Nacional de Parasitología

<sup>2</sup> Available at [www.ncbi.nlm.nih.gov/Genbank](http://www.ncbi.nlm.nih.gov/Genbank).

TABLE I  
Amino acid composition of predicted and trypomastigote-derived mucins of *T. cruzi*

Amino acid	Mature protein composition <sup>a</sup>					Experimental, tGPI-mucin (n = 3)
	Predicted			TcSMUG S (n = 14)	TcSMUG L (n = 8)	
	TcMUC I (n = 15)	TcMUC II (n = 15)	TcMUC III <sup>b</sup> (n = 5)			
	% by frequency ± S.D.					
Ala	5.3 ± 1.9	9.4 ± 1.6	9.5	13.7 ± 1.3	13.3 ± 1.9	6.9 ± 1.7
Cys	0.0	0.0	0.0	0.0	0.0	ND <sup>c</sup>
Asp	1.6 ± 1.0	4.2 ± 1.6	3.1	6.1 ± 1.4	4.2 ± 0.9	ND
Glu	4.4 ± 1.8	8.4 ± 1.4	13.8	6.1 ± 1.4	5.6 ± 1.6	ND
Phe	0.0	0.1 ± 0.3	0.0	0.3 ± 0.7	1.3 ± 0.6	1.0 ± 0.5
Gly	1.1 ± 1.5	<b>8.1 ± 2.1</b>	<b>9.1</b>	6.0 ± 0.8	4.5 ± 1.0	<b>8.4 ± 0.6</b>
His	0.1 ± 0.3	<b>0.7 ± 0.7</b>	0.0	0.0	0.0	<b>0.7 ± 0.3</b>
Ile	3.4 ± 0.9	<b>2.0 ± 1.4</b>	0.0	0.1 ± 0.5	0.1 ± 0.4	<b>2.0 ± 0.6</b>
Lys	<b>5.0 ± 1.0</b>	<b>4.9 ± 1.7</b>	6.8	<b>4.8 ± 1.8</b>	8.6 ± 0.8	<b>4.6 ± 0.6</b>
Leu	0.0	3.3 ± 0.7	0.0	0.0	0.1 ± 0.4	2.5 ± 1.2
Met	0.0	<b>0.7 ± 0.5</b>	0.0	0.0	0.0	<b>0.6 ± 0.5</b>
Asn	1.4 ± 0.8	4.2 ± 1.0	9.1	3.9 ± 0.8	4.1 ± 0.4	ND
Pro	12.0 ± 1.7	<b>9.4 ± 1.7</b>	13.0	6.2 ± 0.9	6.9 ± 0.6	<b>8.7 ± 1.5</b>
Gln	1.2 ± 0.9	4.1 ± 1.9	3.4	5.1 ± 1.4	3.0 ± 0.6	ND
Arg	3.3 ± 0.7	<b>3.1 ± 0.8</b>	0.0	0.1 ± 0.5	0.3 ± 0.5	<b>3.1 ± 0.9</b>
Ser	4.8 ± 1.4	10.9 ± 2.4	20.9	3.0 ± 2.4	6.6 ± 1.9	14.3 ± 4.1
Thr	55.0 ± 3.6	<b>20.2 ± 3.7</b>	10.8	39.8 ± 4.7	38.1 ± 6.9	<b>20.9 ± 0.8</b>
Val	1.1 ± 0.6	5.6 ± 2.1	0.0	3.2 ± 1.3	1.5 ± 0.3	2.3 ± 0.8
Trp	0.0	0.1 ± 0.3	0.0	0.0	0.0	ND
Tyr	0.0	0.1 ± 0.3	0.0	1.7 ± 0.6	1.7 ± 0.8	0.8 ± 0.3
Asx	2.9 ± 1.1	<b>8.4 ± 2.3</b>	12.2	9.9 ± 1.6	<b>8.3 ± 0.8</b>	<b>8.9 ± 0.6</b>
Glx	5.6 ± 1.9	<b>12.5 ± 2.4</b>	17.2	<b>11.1 ± 2.0</b>	9.0 ± 2.4	<b>11.9 ± 1.6</b>

<sup>a</sup> Predicted values similar (within <10% error) to the experimental values are indicated (boldface).

<sup>b</sup> Only TSSA II sequences were analyzed. These sequences show no variation in their amino acid composition, regardless of the strain of *T. cruzi* phylogenetic group II (31).

<sup>c</sup> Not determined.

“Dr. M. Fatała Chaben” (Buenos Aires, Argentina) (31) or kindly provided by Dr. Dimas T. Covas (Fundação Hemocentro de Ribeirão Preto, Ribeirão Preto, São Paulo, Brazil). Additional sera from rabbits and mice infected with different *T. cruzi* isolates were from our own stock (22) or were kindly provided by Dr. Daniel Sánchez (Instituto de Investigaciones Biotecnológicas-Instituto Tecnológico de Chascomús, Universidad Nacional de General San Martín).

**Purification of EMUCT-4-specific Antibodies**—Purified GST-EMUCT-4 protein (1 mg) was immobilized on a N-hydroxysuccinimide-activated column (HiTrap®, Amersham Biosciences) following the manufacturer's guidelines. Five serum samples (100 µl each) of chronic Chagas' disease patients or *T. cruzi* infected rabbits, selected on the basis of their reactivity against GST-EMUCT-4 by ELISA, were pooled and applied to the column, and specific antibodies were purified as described (31).

**Immunoblotting with Purified tGPI-Mucins**—Purified tGPI-mucins (Y strain) were blotted onto nitrocellulose membrane (Hybond-ECL™, Amersham Biosciences) and processed for chemiluminescent immunoblotting as described previously (9).

**Synthetic Peptides and SPOT Assays**—Peptides spanning the consensus sequence (underlined) of the C-terminal peptide of TcMUC II-deduced (TRAPSLRLREIDC) and TcMUC I-deduced (TRAPSSIRRIDC) proteins were custom-synthesized either as free peptides or by the SPOT procedure (Genosys Biotechnologies Inc., The Woodlands, TX) (38). In the latter case, peptides contained one extra N-terminal Thr residue and were devoid of the extra C-terminal Cys residue that enables their chemical coupling to a carrier protein (see above). Additional control SPOT peptides (TTSKAPTPGD and GSLGSSAWACAP) were synthesized on the same filters. Membranes were probed with Chagas' disease sera at 1:100 dilutions as described (31).

**Indirect Immunofluorescence Assay**—Parasites (5–10 × 10<sup>4</sup>) in phosphate-buffered saline were layered onto 3-aminopropyltriethoxysilane-coated round coverslips and processed essentially as described (31). To evaluate the reactivity of intracellular stages (amastigotes, trypomastigotes, and intermediate forms), 10,000 HeLa or Vero cells were plated onto round coverslips 96 h after infection. After 16 h, cells were washed with phosphate-buffered saline, fixed, and processed as described above, with the addition of 0.1% saponin to the blocking and antibody solutions.

## RESULTS

**Amino Acid Composition of Purified tGPI-Mucins**—The amino acid composition of three different batches of purified

tGPI-mucins was determined, rendering homogeneous results (Table I) (9). We compared the average amino acid composition of tGPI-mucins with the predicted amino acid composition of putative mature proteins coded by the TcMUC (groups I–III) and TcSMUG (groups S and L) gene families (Table I). Overall, the average amino acid composition of tGPI-mucins was very similar to that predicted for TcMUC II products (Table I). We tried to determine the N-terminal sequence of the tGPI-mucins by Edman degradation, but no sequence was obtained. One possible explanation is that the N terminus of tGPI-mucins is blocked. Alternatively, the purified tGPI-mucins might be a mixture of gene products, each of them having a different N terminus (see below).

**Mass Spectrometry Analysis of Tryptic Peptides from tGPI-Mucins**—tGPI-mucins were treated with trypsin, and the peptide mixture was analyzed by liquid chromatography-mass spectrometry. Most of the released peptides were glycosylated as determined by selective-ion monitoring at m/z 204 (N-acetylhexosamine) and 292 (N-acetylneuraminic acid) (data not shown). Some of the major glycopeptide ions were submitted to ESI-TOF-MS/MS, giving rise to highly complex spectra that could not be automatically interpreted. When we analyzed non-glycosylated peptide ion species and searched through a homemade data base containing only deduced *T. cruzi* mucin-like sequences, 14 exact hits were obtained (Table II). Most of these peptides (13 of 14) had molecular masses in high agreement (within 0.1 Da tolerance) with the masses of peptides from the central region of different TcMUC II-deduced sequences. Only one peptide had a molecular mass that matched that of a peptide from the hypervariable region of a TcMUC I member (Fig. 1 and Table II). Analysis by ESI-TOF-MS/MS of the most abundant peptide ion species confirmed the peptide mass fingerprinting results (data not shown).

**Mass Spectrometry Analysis of the C Termini of tGPI-Mucins**—The C termini of putative mature protein sequences of distinct *T. cruzi* mucin families and groups are relatively conserved (22, 24, 26), allowing for the identification of 6–7-mer

TABLE II  
Trypomastigote GPI-mucin peptides obtained by trypsin digestion and analyzed by ESI-TOF-MS

For peptide mass fingerprinting analysis, only fully mature *T. cruzi* mucin-deduced sequences were considered. The numbers of sequences analyzed in each mucin family and group were as follows: TcMUC I, 27; TcMUC II, 29; TcMUC III, 9; and TcSMUG S and TcSMUG L, 27. Each sequence was submitted to trypsin autodigest simulation using the BioLynx Protein/Peptide Editor of MassLynx Version 3.5 software. Match parameters were set to  $\pm 0.1$  atomic mass unit for the mass window.

Peptide no.	Ion( <i>m/z</i> )	Charge	Monoisotopic mass		Peptide	Mucin family/group	Clone	CloneGenBank™/EBI accession no.
			Experimental	Predicted				
<i>Da</i>								
1	496.71	+2	991.42	991.45	SDEAAAATEK	TcMUC II	<i>muc153</i>	AAC48354
2	503.30	+1	502.30	502.28	VQEK	TcMUC II	<i>EMUCe-12b9</i>	AAC14217
3	570.26	+2	1138.51	1138.49	GYNEESTPSR	TcMUC II	<i>muc182</i>	AAC48356
4	580.26	+2	1158.52	1158.53	EPGAEQGTNTR	TcMUC II	<i>EMUCe-24m16</i>	AAF44795
5	591.33	+1	590.32	590.29	EESVK	TcMUC II	<i>muc182</i>	AAC48356
6	633.29	+1	632.28	632.31	LSEER	TcMUC II	<i>c2muc1</i>	AY298909 <sup>a</sup>
7	643.31	+2	1284.62	1284.66	EPISGTGGTEPLK	TcMUC II	<i>EMUCt-4</i>	AAK49789, AAC48347
8	648.32	+1	647.31	647.32	TDVGTR	TcMUC II	<i>EMUCe-12p15</i>	AAC14219
9	683.31	+2	1364.62	1364.67	TTPHPQSSATPNK	TcMUC II	<i>EMUCe-12b9</i>	AAC14217
10	697.30	+1	696.30	696.30	GNNPPAK	TcMUC II	<i>c2muc2</i>	AY298909 <sup>a</sup>
11	703.35	+1	702.34	702.32	SPEQDK	TcMUC II	<i>muc-ra2</i>	AAC46908
12	737.84	+2	1473.70	1473.68	ANGVDEQVAPDMTK	TcMUC II	<i>muc-ra1</i>	AAC46907
13	805.40	+1	804.39	804.40	VTASGDQK	TcMUC I	<i>muc-loc5</i>	AAK94015
14	887.45	+1	886.44	886.41	TSTEHANK	TcMUC II	<i>EMUCe-15l12</i>	AAC14223

<sup>a</sup> Cosmid number; sequence not yet available in the GenBank™/EBI Data Bank.

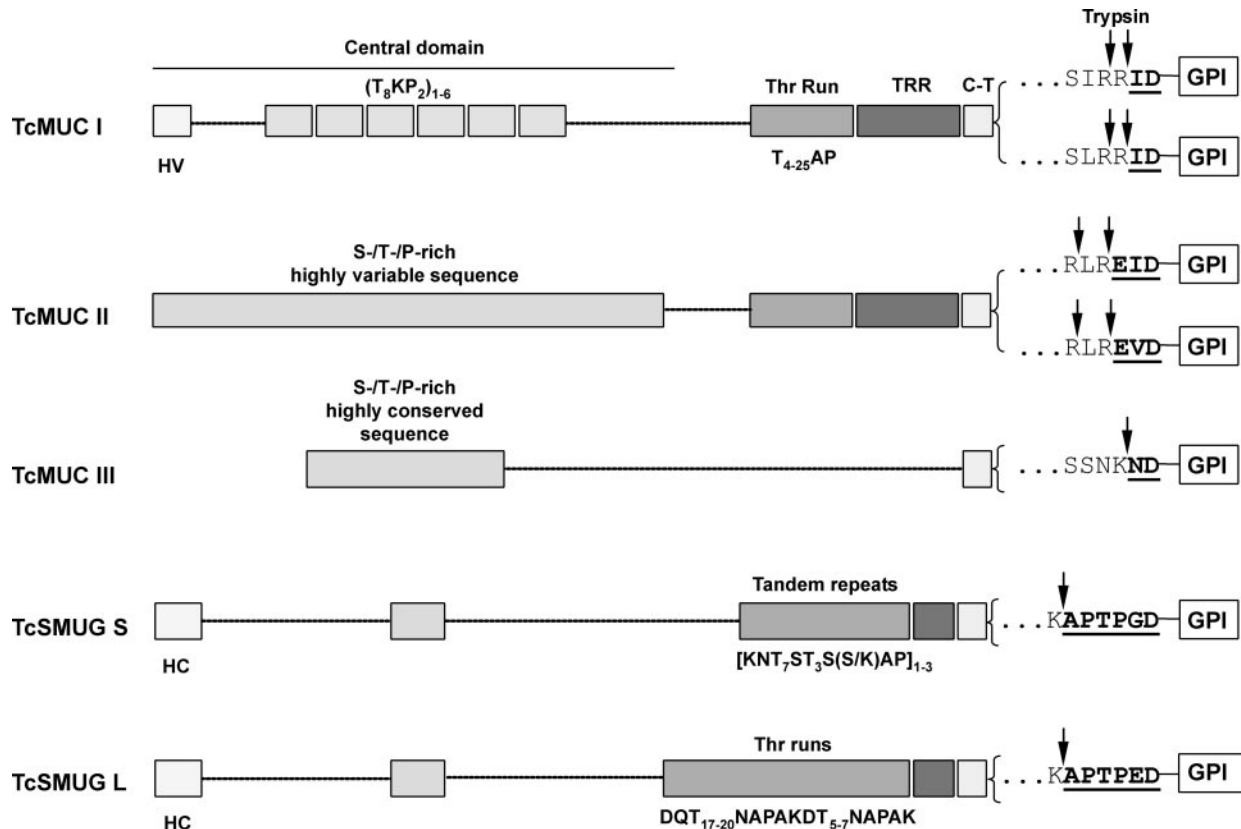


FIG. 1. Schematic representation of *T. cruzi* TcMUC and TcSMUG families and groups, highlighting their consensus C-terminal peptides. The general arrangement of the mature protein of each mucin family and group is illustrated according to Frasch (14), with a few modifications. The 6–7-mer peptide sequence located at the C terminus and its putative trypsin digestion site(s) (arrows) and released peptide (underlined) are indicated. The GPI moiety is attached to the C-terminal aspartic acid residue, as previously shown for trypomastigote and epimastigote mucins (19). HV, hypervariable N terminus; HC, highly conserved N terminus; TRR, Thr-rich region; C-T, C terminus.

consensus or signature peptides, which can be defined as S(I/L)RRID for TcMUC I, RLRE(I/V)D for TcMUC II, SSNKND for TcMUC III, and KAPTPGD and KAPTPED for TcSMUG S and TcSMUG L, respectively (Fig. 1). Because all of them are likely to be linked to a GPI anchor through the highly conserved Asp residue (19), we foresaw that the GPI-peptides released after trypsin treatment would provide a valuable tool for the characterization of tGPI-mucins (Fig. 1). tGPI-peptides were sepa-

rated from free peptides and glycopeptides by octyl-Sepharose and analyzed by negative-ion mode ESI-TOF-MS (Fig. 2). The fraction eluted with 20% 1-propanol showed a series of triply ( $[M - 3H]^{3-}$ ) and doubly ( $[M - 2H]^{2-}$ ) charged negative-ion species at *m/z* 700–1500. Three major doubly charged ion species were observed at *m/z* 1088, 1108, and 1109 (Fig. 2A). A series of ions seemed to be derived from these ions by the addition or subtraction of either hexose (Hex; *m/z* difference of

81) or aminoethylphosphonate ( $m/z$  difference of 54) residues. Some of the other ion species observed in the ESI-TOF-MS spectrum (Fig. 2A) seem to be sodium or ammonium ion adducts or dehydrated species related to the major GPI-peptide series. The remaining minor GPI-peptides were not further analyzed. The ion at  $m/z$  1108 ( $[M - 2H]^{2-} = 1107.88$ , molecular mass of 2217.76 Da) could be tentatively assigned to a structure composed of EID-(ethanolamine phosphate)-Hex<sub>4</sub>-(aminoethylphosphonate)-HexN-*myo*-inositol-P-alkylacylglycerol(C16:0/C18:2), with a predicted monoisotopic molecular mass of 2217.00 Da. The ion at  $m/z$  1109 ( $[M - 2H]^{2-} = 1108.87$ , molecular mass of 2219.74 Da) could be tentatively assigned to a structure composed of EID-(ethanolamine phosphate)-Hex<sub>4</sub>-(aminoethylphosphonate)-HexN-*myo*-inositol-P-alkylacylglycerol(C16:0/C18:1), with a predicted monoisotopic molecular mass of 2219.02 Da. Therefore, the difference between the ions species at  $m/z$  1108 and 1109 could be attributed to the presence of a double bond in the fatty acid chain. The ion at  $m/z$  1088 ( $[M - 2H]^{2-} = 1088.34$ , molecular mass of 2178.68 Da) could be assigned to a structure containing EVD-(ethanolamine phosphate)-Hex<sub>4</sub>-(aminoethylphosphonate)-HexN-*myo*-inositol-P-alkylacylglycerol(C16:0/C16:0), with a predicted monoisotopic molecular mass of 2178.96 Da. It is worth noting that the ions at  $m/z$  1108, 1109, and 1088 apparently have a GPI composition identical to that described previously for the major species of tGPI-mucins (19). More important, the sequences of the peptide portion of the ions at  $m/z$  1088 and 1108/1109 (EVD and EID, respectively) correspond to two possible mature C-terminal signature peptides predicted for TcMUC II (Fig. 1).

The putative composition of the major GPI-peptide ion at  $m/z$  1108 was further addressed by ESI-TOF-MS/MS (Fig. 2B). The spectrum showed two major daughter ions at  $m/z$  2109/2110 and 1752, possibly corresponding to the fragments EID-GPI<sup>-ap</sup> and GPI<sup>-ap</sup>, respectively, which both lack the aminoethylphosphonate (ap) residue. The remaining ions could be assigned to GPI-peptide- or GPI-derived fragments. Among them, several characteristic GPI-derived ions were observed at  $m/z$  79 (PO<sub>3</sub><sup>-</sup>), 124 (aminoethylphosphonate), 140 (ethanolamine phosphate), 241 (*myo*-inositol cyclic phosphate), 279 (carboxylate ion of C18:2), 377 (monoalkylglycerophosphatidylinositol), and 819 (alkylacylglycerophosphatidylinositol) (Fig. 2B). Assignments for the major daughter ions and a putative structure for the major tGPI-peptide species are presented in Fig. 2C. Taken together, the amino acid composition and mass spectrometry results strongly indicate that TcMUC II genes encode most of the tGPI-mucins.

**TcMUC II Products Are Expressed in the Mammal-dwelling Stages**—To study the *in vivo* expression pattern of TcMUC II products, we immunized groups of mice with the entire putative mature product (as predicted in Ref. 22) encoded by three different members of this group (*EMUCt-4*, *c2muc1*, and *c2muc3*) expressed in *Escherichia coli* as GST fusion proteins. We also immunized groups of mice with GST fusion proteins spanning solely the variable central domain of each member. All of these antisera recognized the corresponding immunogen expressed in bacteria as His-tagged fusion proteins (data not shown). We carried out indirect immunofluorescence assays with permeabilized *T. cruzi* infected HeLa or Vero cells, containing a mixture of amastigotes, trypomastigotes, and intermediate forms. All intracellular parasite forms were labeled by the antisera raised against the full-length *c2muc1* constructs, with trypomastigotes rendering the strongest signal (Fig. 3, A and B). None of the antisera raised against the central domains labeled the intracellular parasite forms (data not shown).

To further assess the specificity of these results, anti-EMUCt-4 antibodies were affinity-purified from sera of chronic

Chagas' disease patients and *T. cruzi* infected rabbits using the full-length construct as a bait. Mammalian cell-derived trypomastigotes and amastigotes were clearly labeled by these antibodies in indirect immunofluorescence assays (Fig. 3, C and D), whereas axenic culture-derived insect parasite stages (epimastigotes and metacyclic trypomastigotes) gave no signal by this technique (data not shown). In a second set of experiments, affinity-purified anti-EMUCt-4 antibodies were probed against permeabilized infected cells as described above. The pattern of labeling was very similar to that displayed by our panel of antisera raised against full-length recombinant TcMUC II proteins (Fig. 3, E and F). We then probed the purified tGPI-mucins by Western blotting using antisera raised against different TcMUC II central regions or full-length constructs or against the consensus C-terminal peptide. The two latter antisera rendered homogeneous results, highlighting a broad smear ranging from ~60 to ~220 kDa (Fig. 4, lanes 1, 3, and 5), typical of tGPI-mucins (6, 7, 9). The same pattern was obtained when tGPI-mucins were probed with a serum pool or purified anti- $\alpha$ -galactosyl antibody from chronic Chagas' disease patients (Fig. 4, lanes 7 and 8). On the other hand, only discrete and faint bands were revealed by some of the antisera raised against TcMUC II central regions (Fig. 4, lanes 4 and 6). Altogether, these results indicate that proteins encoded by TcMUC II genes are expressed on the surface of the mammalian parasite stages, preferentially in cell-derived trypomastigotes, and that they co-purify with tGPI-mucins.

**Mapping of TcMUC II B-cell Peptide Epitopes Recognized during *T. cruzi* Infections**—Our results using affinity-purified anti-GST-EMUCt-4 antibodies from sera of infected mice indicated that the protein backbone of TcMUC II products does elicit an *in vivo* humoral immune response during *T. cruzi* infections (Fig. 4). This broad-range reactivity might be attributed either to immunological cross-reactivity with other TcMUC II mucins or to a differential glycosylation pattern of the same gene product. To map the EMUCt-4 B-cell peptide epitope(s), we constructed truncated versions of the mature full-length sequence (Fig. 5A). These variants encompassed solely the central region and the central region plus the Thr run, respectively. The different constructs were expressed in *E. coli* as C-terminal GST fusions, purified, and tested by ELISA. Sera obtained from animals infected with different parasite stocks or from chronic Chagas' disease patients poorly recognized both the variable central region and the Thr run, with a seroprevalence of 5–25% (Fig. 5B). However, the recognition was greatly enhanced when the full-length recombinant protein was assayed (>10-fold increase in the recorded absorbance values) (data not shown). The seroprevalence recorded in this case was also significantly increased, with values of 59, 47, and 75% for human Chagas' disease sera, infected mouse sera, and infected rabbit sera, respectively (Fig. 5B). Similar results were obtained when different GST fusions spanning truncated versions of the *c2muc1* and *c2muc3* products were analyzed (data not shown). Western blots probed with chronic Chagas' disease sera were in the same line. As shown in Fig. 5C, although some of the variable central regions (EMUCe-8, *c2muc1*, EMUCt-4, and EMUCe-12b9 (lanes 4, 5, 7, and 8, respectively)) rendered a weak signal, this reactivity was greatly amplified when the corresponding mature full-length sequences were evaluated under the same conditions (lane 6). Unexpectedly, recombinant mucins encompassing either the central domain or the full-length sequence showed two to four reactive bands on the blot (lanes 4–8). Possibly, this could be a result of proteolytic degradation because it had not been observed with the freshly purified recombinant proteins (data not shown).

The C-terminal sequence from both TcMUC I- and II-de-

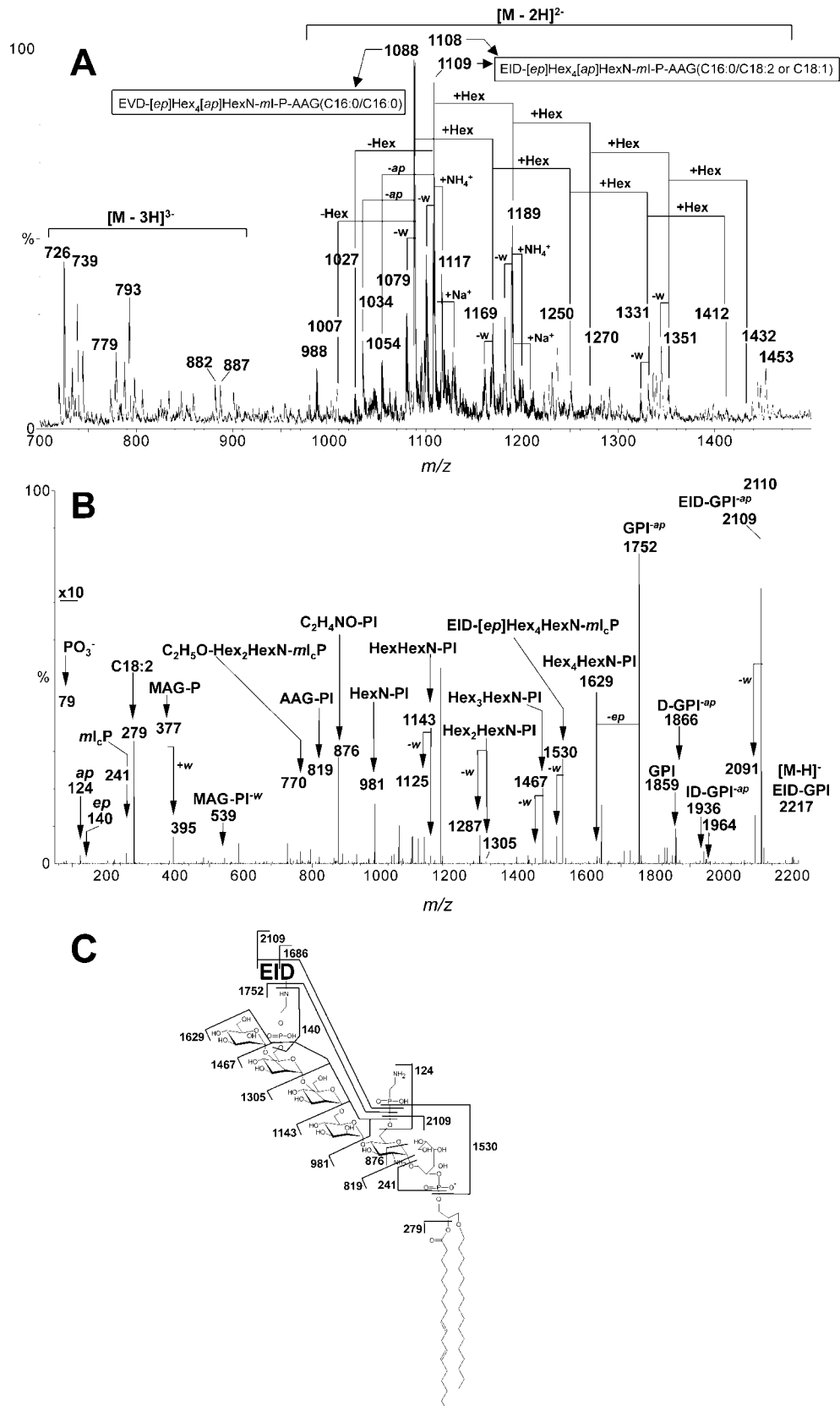


**FIG. 2. ESI-TOF-MS (negative-ion mode) analysis of tGPI-peptides.** A, ESI-TOF-MS spectrum. *w*, water; *ep*, ethanolamine phosphate; *ap*, aminoethylphosphonate; *ml*, *myo*-inositol; *P*, phosphate; *AAG*, 1-*O*-alkyl-2-*O*-acylglycerol. B, deconvoluted ESI-TOF-MS/MS spectrum of the ion at *m/z* 1108.4. For simplicity, the original spectrum containing singly, doubly, and triply charged ion species was deconvoluted to a spectrum depicting only singly charged ion species using the MaxEnt 3 function of MassLynx Version 3.5 software. *ml<sub>c</sub>P*, *myo*-inositol cyclic phosphate; *MAG-P*, 1-*O*-C16:0-monoalkylglycero-3-phosphate; *MAG-PI*, 1-*O*-C16:0-monoalkylglycero-3-phospho-*myo*-inositol; *AAG-PI*, 1-*O*-C16:0-alkyl-2-*O*-C18:2-acylglycerol-3-phospho-*myo*-inositol; *HexN-PI*, hexosamine-phosphatidylinositol; *GPI*, EID-(ethanolamine phosphate)-Hex<sub>4</sub>-(aminoethylphosphonate)-HexN-alkylacylglycerophosphatidylinositol; *GPI<sup>-ap</sup>*, *GPI* minus the aminoethylphosphonate residue. C, proposed ESI-TOF-MS/MS assignments and putative structure of the major tGPI-peptide ion species at *m/z* 1108.

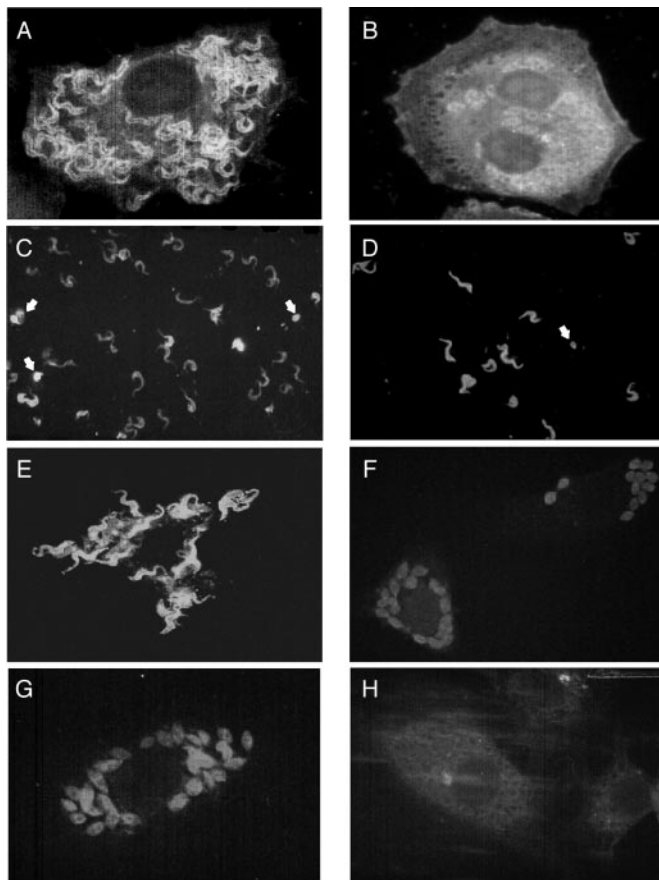


**FIG. 3. Stage expression of TcMUC II products.** A and B, saponin-permeabilized *T. cruzi* infected Vero cells probed with anti-GST-c2muc1 antibodies from an immunized mouse, showing intracellular trypomastigote and amastigote forms, respectively (magnification  $\times 180$  under UV light); C and D, non-permeabilized amastigotes (indicated by arrows), cell-derived trypomastigotes, and intermediate forms probed using anti-GST-EMUCt-4 antibodies purified from Chagas' disease patients and *T. cruzi* infected rabbit sera, respectively; E and F, saponin-permeabilized infected HeLa cells probed with anti-GST-EMUCt-4 antibodies purified from Chagas' disease sera and *T. cruzi* infected rabbit sera, respectively; G and H, saponin-permeabilized *T. cruzi* infected Vero cells probed with mouse anti-GST-c2muc1 antibodies pretreated with the consensus C-terminal peptides of TcMUC I (TTRAPSSIRRID) and TcMUC II (TTRAPSRLREID), respectively.

duced proteins is highly conserved (Fig. 1). Comparison of these consensus sequences, S(I/L)RRRID for TcMUC I and RLRE(I/V)D for TcMUC II, showed only two amino acid differences (underlined). It was therefore possible that both C-terminal peptides display antigenic cross-reactivity. To address this issue, a series of immobilized 12-mer peptides derived from either TcMUC I or II C-terminal sequences were synthesized (Fig. 6A). Filters were probed with three human chronic Chagas' disease sera, and all of them highlighted the peptide spanning the consensus sequence of the TcMUC II group. Conversely, none of these sera reacted against the consensus C-terminal peptide of the TcMUC I group or against the control peptides, including the consensus C-terminal region of the TcSMUG family (group S) and one peptide derived from the GPI anchorage signal of the TcMUC II group, unlikely to be present in the mature proteins (22). We also evaluated the ability of TcMUC I and TcMUC II C-terminal soluble peptides to inhibit the recognition of the GST-tagged full-length EMUCt-4 construct by selected sera or antibody fractions. The TcMUC I C-terminal peptide generally displayed negligible inhibition (even at 100  $\mu\text{g/ml}$ ) of the binding of affinity-purified anti-EMUCt-4 antibodies and sera from infected rabbits and chronic

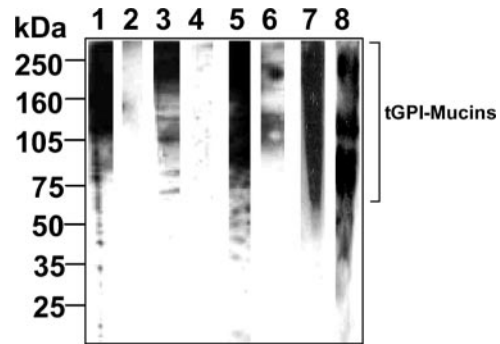


**FIG. 4. Antibodies to recombinant TcMUC II constructs recognize purified tGPI-mucins.** Purified tGPI-mucins blotted onto nitrocellulose membrane were sequentially incubated with the indicated antibodies or antisera, followed by biotinylated anti-IgG antibody, horseradish peroxidase-conjugated streptavidin, and chemiluminescent reagent (9). Lane 1, mouse antiserum against the TcMUC II consensus C-terminal peptide; lane 2, mouse antiserum against the TcMUC I consensus C-terminal peptide; lane 3, mouse antiserum against the GST-tagged full-length c2muc1 protein; lane 4, mouse antiserum against the GST-EMUCt-4 central domain (no C terminus); lane 5, mouse antiserum against the GST-tagged full-length EMUCt-4 protein; lane 6, mouse antiserum against the GST-c2muc3 central domain (no C terminus); lanes 7 and 8, serum pool and anti- $\alpha$ -galactosyl antibodies from human chronic Chagas' disease patients, respectively (positive controls). The relative molecular masses of protein standards are indicated on the left. The characteristic broad-range immunoreactivity of tGPI-mucins (9) is indicated on the right.

Chagas' disease patients. By contrast, complete inhibition was achieved by the TcMUC II C-terminal peptide at 4–20  $\mu\text{g/ml}$  (Fig. 6B). This specific inhibition was further confirmed by indirect immunofluorescence assays with permeabilized infected cells, in which the reaction of an antiserum raised against the GST-tagged full-length c2muc1 construct was abolished by its preincubation with a molar excess of the consensus TcMUC II C-terminal peptide, but not by the TcMUC I one (Fig. 3, G and H). Finally, an antiserum raised against the TcMUC II consensus peptide, but not one raised against the TcMUC I one, recognized the tGPI-mucins by Western blotting (Fig. 4, lanes 1 and 2). Taken together, our data indicate that the protein backbone of TcMUC II products elicits antibody responses during *T. cruzi* infection, mainly driven toward the epitope(s) contained within the C-terminal peptide conserved throughout this group.

#### DISCUSSION

Multigene families constitute a substantial part of the overall genome content in all organisms where they were found. Those involved in housekeeping functions, such as the ribosomal and transfer RNA genes, usually show limited heterogeneity. In contrast, the generation and accumulation of multiple related genes displaying different expression patterns and/or coding for proteins with subtly altered sequences/specificities seem to be a common evolutionary trend for the adaptation of the organisms to changing or hostile environmental conditions. *T. cruzi* contains a vast array of mucin-like genes that have been classified into two main families, TcSMUG and TcMUC, which together account for >1% of the parasite genome (reviewed in Ref. 27). Besides the presence of two groups, the TcSMUG family displays no major intragroup sequence variability, which is consistent with its expression in the insect vector, where no adaptive immune system is present (24).<sup>3</sup> In contrast, the TcMUC gene family is composed of a larger number of members (approximately an order of magnitude higher than that of TcSMUG) showing substantial variability (22).

<sup>3</sup> I. C. Almeida, unpublished data.

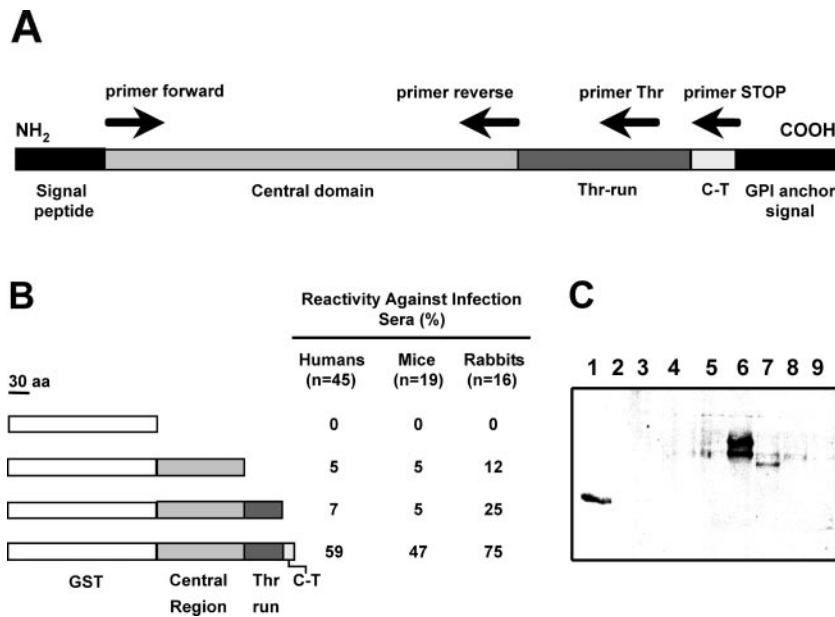


**FIG. 5. Recognition of recombinant TcMUC II mucins by sera from *T. cruzi* infected humans and animals.** *A*, the diagram shows the modular structure of TcMUC II-deduced mucins. The oligonucleotides used to amplify different protein variants are indicated above. *C-T*, C terminus. *B*, the indicated variants of GST-EMUCt-4 protein were probed by ELISA with a panel of sera collected from human Chagas' disease patients or *T. cruzi* infected mice and rabbits at a 1:500 dilution. *aa*, amino acids. *C*, GST fusion proteins containing the central region of different TcMUC II mucins (except for lane 6) were resolved by SDS-PAGE and transferred onto nitrocellulose membrane. The membrane was probed with a chronic Chagas' disease serum (1:1000 dilution) and revealed with the addition of secondary antibodies coupled to peroxidase, followed by chemiluminescent reagent. The relative molecular mass markers (in kilodaltons) are indicated on the right. Lane 1, GST-TSSA II (positive control) (31); lane 2, GST-c2muc3; lane 3, GST-c2muc2; lane 4, GST-EMUCe-8; lane 5, GST-c2muc1; lane 6, GST-full-length EMUCt-4; lane 7, GST-EMUCt-4; lane 8, GST-EMUC-12b9; lane 9, GST.

The variability is largely restricted to the hypervariable region in the TcMUC I group and to the entire central domain in TcMUC II genes by means of yet undefined mechanisms. This genetic complexity along with other indirect evidence (22, 23, 28) led to the speculation that the TcMUC products code for the parasite mucins displayed on the surface of the mammal-dwelling stages.

Our present data not only demonstrate this assumption, but also identify the TcMUC II products as the major component of the tGPI-mucins. The overall amino acid composition (Table I) and the mass spectrometry analysis of peptides released after trypsin digestion of purified tGPI-mucins (Table II) are consistent with this idea. In addition, the characterization of the tryptic peptides that remained attached to GPI allowed us to identify two sequences corresponding to the predicted mature C terminus of the TcMUC II group (Fig. 1). It is noteworthy that these two peptides (EID and EVD) were linked to different GPI moieties (Fig. 2). It remains to be studied whether these different glycolipid moieties confer distinct structural and/or functional properties (*i.e.* intramembrane lateral motility, shedding) to the ensuing mucins. The composition of the GPI glycan attached to both peptides was identical to that described previously for the major species of tGPI-mucins (19). More important, we found several tryptic non-glycosylated peptides matching sequences of different TcMUC II-deduced products (Table II), further stressing the identity of the coat. In sharp contrast to other protozoan parasites (39, 40), our results indicate that *T. cruzi* trypomastigotes present a heterogeneous surface coat to the mammalian host, which might constitute a parasite strategy to evade host immune surveillance (see below).

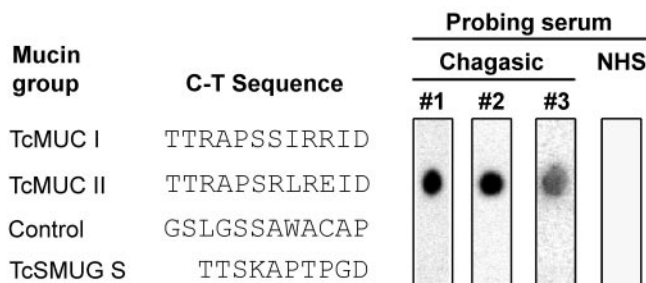
Our immunological evidence further supports the predominance of TcMUC II products in tGPI-mucins. As shown in Figs. 3 and 4, infection and immunization antibodies against full-length recombinant TcMUC II products labeled the surface of trypomastigotes and also recognized a preparation of tGPI-

mucins. Furthermore, an antiserum raised against the consensus C-terminal peptide deduced from the TcMUC II group recognized the tGPI-mucins by Western blotting, whereas an antiserum raised against the TcMUC I C-terminal peptide failed to do so (Fig. 4). In addition to trypomastigote forms, immunization and infection antibodies directed against full-length TcMUC II products labeled the surface of intracellular amastigotes and intermediate forms (Fig. 3), although the signal was weaker. These results suggest that TcMUC II products might also form part of the surface coat of these parasite stages. Although more refined analyses are required to ascertain this assumption, it is worth mentioning that certain biochemical and immunochemical similarities between cell-derived trypomastigote and amastigote mucins have been noted (7).

We have previously shown that the majority of the humoral immune response of chronic Chagas' disease patients against the tGPI-mucins is directed against  $\alpha$ -galactosyl epitopes present on their *O*-linked oligosaccharides (9). More recently, we observed that treatment of tGPI-mucins with  $\alpha$ -galactosidase abolished most (60–90%), but not all, of the reactivity of individual human Chagas' disease sera against these glycolipoproteins.<sup>3</sup> These results might be explained by the existence of additional, non-carbohydrate epitope(s) in tGPI-mucins. As shown in Fig. 5, sera collected from three different species of mammals infected with *T. cruzi* recognized the TcMUC II products expressed in bacteria, thus devoid of any kind of glycosylation. We mapped this reactivity using these sera and verified that it was directed against a C-terminal peptide, highly conserved throughout this group of molecules (Figs. 5 and 6). One of the major concerns regarding these assays was the putative existence of antibodies directed against the consensus C-terminal peptide of the TcMUC I group that could cross-react with the highly related TcMUC II C-terminal sequence (Fig. 1). We have demonstrated, however, that both peptides do not cross-react and that the C-terminal peptide of the TcMUC II group, unlike that of TcMUC I, elicits an anti-



A



B

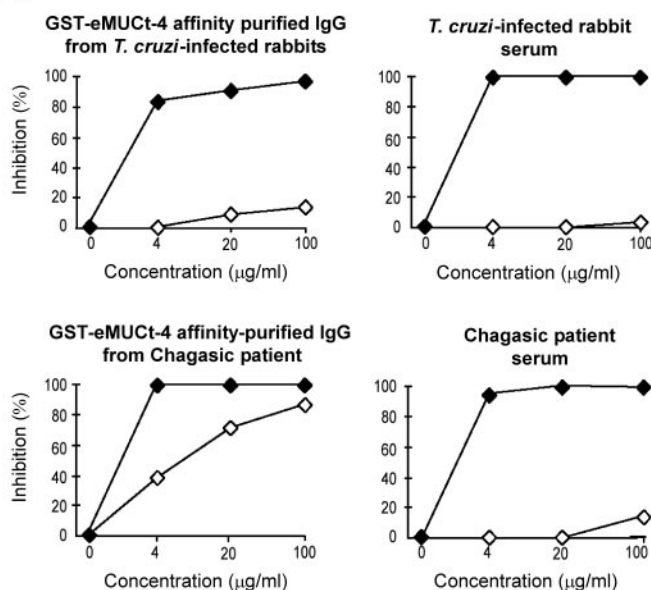


FIG. 6. Specificity of antibodies from Chagas' disease patients directed against TcMUC II products. A, shown is the reactivity of three independent human Chagas' disease sera and one normal human serum (NHS) against the indicated peptides synthesized by the SPOT procedure. Sera were tested at a 1:100 dilution and revealed as indicated in the legend to Fig. 5. C-T, C-terminal. B, ELISA plates coated with the GST-tagged full-length EMUCt-4 protein (100 ng/well) were processed with the antiserum indicated at the top of each panel. Prior to the assay, affinity-purified antibodies and sera were incubated for 30 min with the indicated amounts of bovine serum albumin-coupled peptides spanning the C-terminal sequence of TcMUC I ( $\diamond$ ) or TcMUC II ( $\blacklozenge$ ).

body response during infection (Figs. 4–6). Because of its prevalence (on a molar basis) at the surface coat of the mammal-dwelling stages, this sequence might provide a target for protective immune responses.

One striking finding was that multiple antisera against the central region of TcMUC II products did not label the parasite by indirect immunofluorescence assays and reacted faintly when probed by Western blotting with total tGPI-mucins (Fig. 4) (data not shown). This result correlates with the humoral response in *T. cruzi* infected animals and humans (Fig. 5), which did not elicit a strong antibody reaction to the variable central regions of TcMUC II. Despite this, the central region of TcMUC II products does contain B-cell epitopes (data not shown). Moreover, the antibody repertoire in animals immunized with the full-length recombinant constructs was not exclusively directed against the C-terminal peptide (data not shown), suggesting that the bias observed *in vivo* in the antibody generation against TcMUC II involved additional mechanisms. One possibility is that TcMUC II central peptide re-

gions are shielded *in vivo* by post-translational modifications (mainly O-glycosylation) (data not shown) and are thus not directly exposed to the immune system. This would also explain the lack of reactivity of our antisera raised against TcMUC II central regions. Furthermore, the masking of the TcMUC II variable central domain by O-linked oligosaccharides (9) (data not shown) might interfere in the processing and presentation of internal mucin glycopeptides by major histocompatibility complex molecules, as previously noticed for other glycopeptides (41). The variability of the central domain might also weaken the chances of accumulation of putative major histocompatibility complex ligands inside the infected cell.

In addition, since the huge diversity found in the central regions of TcMUC II seems indeed to be present in the mature products, a role for these molecules in immunoevasion can be envisaged. As demonstrated in other systems, the simultaneous display of multiple related epitopes on the surface of a pathogen brings about significant consequences on the immune response mounted by the host (42, 43). Although speculative, such a mechanism might contribute to the lack of *in vivo* reactivity toward TcMUC II variable regions during *T. cruzi* infections. However, a puzzling aspect of the variable central regions that does not favor their role in an immunoevasion mechanism is their heavy glycosylation involving immunodominant ( $\alpha$ -galactosyl) epitopes, unless there is a significant number of these TcMUC II mucins poorly glycosylated or lacking glycosylation. These two apparently conflicting hypotheses need now to be carefully addressed.

In conclusion, the vast majority of the mucin molecules present on the surface of the cell-derived trypomastigotes (and likely also amastigotes) belong to the TcMUC II group. A minor proportion of TcMUC I products in tGPI-mucins cannot, however, be ruled out. In fact, the sequence of 1 of 14 of the analyzed trypsin-released peptides matched a TcMUC I product (Table II). The definitive temporal and subcellular localization of the products encoded by this group remains uncertain. The presence of a hypervariable region highly exposed to the extracellular milieu in TcMUC I-deduced sequences constitutes an attractive way of undermining the adaptive immune response, as postulated above for the TcMUC II group. In addition, circulating antibodies directed against these hypervariable regions were detected in *T. cruzi* infected humans and animals (28),<sup>4</sup> suggesting that these sequences are indeed exposed to the mammalian immune system. One interesting possibility is that TcMUC I products are expressed by the mammal-dwelling stages, but are barely detected because they are prone to massive shedding to the medium either by cleavage of their GPI anchor (28) or by their differential partition into released vesicles (44) or membrane-bound trails (45). Further studies are required to address the expression pattern of TcMUC I products and to clarify the *in vivo* biological function and immunological implications of TcMUC II diversity.

**Acknowledgments**—We are indebted to Drs. Luiz R. Travassos (Universidade Federal de São Paulo, São Paulo, Brazil), Alvaro Acosta-Serrano (University of Glasgow, Glasgow, Scotland, United Kingdom), and Julio Scharfstein (Universidade Federal de Rio de Janeiro, Rio de Janeiro, Brazil) for critical reading of the manuscript, valuable suggestions, and continuous encouragement. We thank Francisco Leocata for assistance in some experiments, Lilianna Sferco and Berta Franke de Cazzulo (Instituto de Investigaciones Biotecnológicas-Instituto Tecnológico de Chascomús) for the parasites, Fabio Fraga (Instituto de Investigaciones Biotecnológicas-Instituto Tecnológico de Chascomús) for care and maintenance of the animals, and Dr. Ramiro E. Verdun (Instituto de Investigaciones Biotecnológicas-Instituto Tecnológico de Chascomús) for expert advice on microscopy. We are grateful to Dr.

<sup>4</sup> V. A. Campo, C. A. Buscaglia, J. M. Di Noia, and A. C. C. Frasch, unpublished data.

Antonio C. M. Camargo (Instituto Butantan, São Paulo, Brazil) for full access to the Center for Applied Toxinology-Centro de Excelência em Pesquisa e Difusão Proteômica Facility; Iain Campuzano, Joerg von Helden, and Juarez A. Silveira (Waters Micromass Ltd.) for access to the capillary HPLC-Q-tof in the initial experiments; Douglas Lamont (University of Dundee) for expert assistance with ESI-TOF-MS; and S. J. Tadeu and Dr. R. A. Maldonado-Medina for continuous support.

## REFERENCES

- World Health Organization (2002) *WHO Tech. Rep. Ser.* **905**, 1–109
- Tyler, K. M., and Engman, D. M. (2001) *Int. J. Parasitol.* **31**, 472–481
- Alves, M. J., and Colli, W. (1975) *FEBS Lett.* **52**, 188–190
- Yoshida, N., Mortara, R. A., Araguth, M. F., Gonzalez, J. C., and Russo, M. (1989) *Infect. Immun.* **57**, 1663–1667
- Schenkman, S., Ferguson, M. A. J., Heise, N., Cardoso de Almeida, M. L., Mortara, R. A., and Yoshida, N. (1993) *Mol. Biochem. Parasitol.* **59**, 293–303
- Almeida, I. C., Krautz, G. M., Krettli, A. U., and Travassos, L. R. (1993) *J. Clin. Lab. Anal.* **7**, 307–316
- Almeida, I. C., Ferguson, M. A. J., Schenkman, S., and Travassos, L. R. (1994) *Braz. J. Med. Biol. Res.* **27**, 443–447
- Previato, J. O., Jones, C., Goncalves, L. P., Wait, R., Travassos, L. R., and Mendonça-Previato, L. (1994) *Biochem. J.* **301**, 151–159
- Almeida, I. C., Ferguson, M. A. J., Schenkman, S., and Travassos, L. R. (1994) *Biochem. J.* **304**, 793–802
- Serrano, A. A., Schenkman, S., Yoshida, N., Mehlert, A., Richardson, J. M., and Ferguson, M. A. J. (1995) *J. Biol. Chem.* **270**, 27244–27253
- Pereira-Chioccola, V. L., Acosta-Serrano, A., Correia de Almeida, I., Ferguson, M. A. J., Souto-Padron, T., Rodrigues, M. M., Travassos, L. R., and Schenkman, S. (2000) *J. Cell Sci.* **113**, 1299–1307
- Previato, J. O., Jones, C., Xavier, M. T., Wait, R., Travassos, L. R., Parodi, A. J., and Mendonça-Previato, L. (1995) *J. Biol. Chem.* **270**, 7241–7250
- Van Klinken, B. J., Dekker, J., Buller, H. A., and Einerhand, A. W. (1995) *Am. J. Physiol.* **269**, G613–G627
- Frasch, A. C. C. (2000) *Parasitol. Today* **16**, 282–286
- Almeida, I. C., and Gazzinelli, R. T. (2001) *J. Leukocyte Biol.* **70**, 467–477
- Acosta-Serrano, A., Almeida, I. C., Freitas-Junior, L. H., Yoshida, N., and Schenkman, S. (2001) *Mol. Biochem. Parasitol.* **114**, 143–150
- Andrews, N. W., Hong, K. S., Robbins, E. S., and Nussenzweig, V. (1987) *Exp. Parasitol.* **64**, 474–484
- Schenkman, S., Jiang, M. S., Hart, G. W., and Nussenzweig, V. (1991) *Cell* **65**, 1117–1125
- Almeida, I. C., Camargo, M. M., Procopio, D. O., Silva, L. S., Mehlert, A., Travassos, L. R., Gazzinelli, R. T., and Ferguson, M. A. J. (2000) *EMBO J.* **19**, 1476–1485
- Di Noia, J. M., Sanchez, D. O., and Frasch, A. C. C. (1995) *J. Biol. Chem.* **270**, 24146–24149
- Salazar, N. A., Mondragon, A., and Kelly, J. M. (1996) *Mol. Biochem. Parasitol.* **78**, 127–136
- Di Noia, J. M., D'Orso, I., Aslund, L., Sanchez, D. O., and Frasch, A. C. C. (1998) *J. Biol. Chem.* **273**, 10843–10850
- Freitas-Junior, L. H. G., Briones, M. R. S., and Schenkman, S. (1998) *Mol. Biochem. Parasitol.* **93**, 101–114
- Di Noia, J. M., D'Orso, I., Sanchez, D. O., and Frasch, A. C. C. (2000) *J. Biol. Chem.* **275**, 10218–10227
- Allen, C. L., and Kelly, J. M. (2001) *Exp. Parasitol.* **97**, 173–177
- Campo, V., Di Noia, J. M., Buscaglia, C. A., Agüero, F., Sánchez, D. O., and Frasch, A. C. C. (2004) *Mol. Biochem. Parasitol.* **133**, 81–91
- Di Noia, J. M., D'Orso, I., and Frasch, A. C. C. (2002) in *Molecular Mechanisms in the Pathogenesis of Chagas' Disease* (Kelly, J. M., ed) pp. 31–56, Landes Bioscience, Georgetown, Washington, D. C.
- Pollewick, G. D., Di Noia, J. M., Salto, M. L., Lima, C., Leguizamon, M. S., de Lederkremer, R. M., and Frasch, A. C. C. (2000) *J. Biol. Chem.* **275**, 27671–27680
- Agüero, F., Verdun, R. E., Frasch, A. C. C., and Sanchez, D. O. (2000) *Genome Res.* **10**, 1996–2005
- Previato, J. O., Sola-Penna, M., Agrellos, O. A., Jones, C., Oeltmann, T., Travassos, L. R., and Mendonça-Previato, L. (1998) *J. Biol. Chem.* **273**, 14982–14988
- Di Noia, J. M., Buscaglia, C. A., De Marchi, C. R., Almeida, I. C., and Frasch, A. C. C. (2002) *J. Exp. Med.* **195**, 401–413
- Buscaglia, C. A., and Di Noia, J. M. (2003) *Microbes Infect.* **5**, 419–427
- Zingales, B., Pereira, M. E., Oliveira, R. P., Almeida, K. A., Umezawa, E. S., Souto, R. P., Vargas, N., Cano, M. I., da Silveira, J. F., Nehme, N. S., Morel, C. M., Brener, Z., and Macedo, A. (1997) *Acta Trop.* **68**, 159–173
- Andrews, N., and Colli, W. (1982) *J. Protozool.* **29**, 264–269
- Ferguson, M. A. J. (1993) in *Glycobiology: A Practical Approach* (Fukuda, M., and Kobata, A., eds) pp. 349–383, Oxford University Press, New York
- Hendrickson, R. L., and Meredith, S. C. (1984) *Anal. Biochem.* **136**, 65–74
- Buscaglia, C. A., Campetella, O., Leguizamon, M. S., and Frasch, A. C. C. (1998) *J. Infect. Dis.* **177**, 431–436
- Frank, R., and Doring, R. (1988) *Tetrahedron* **44**, 6031–6040
- Borst, P., and Fairlamb, A. H. (1998) *Annu. Rev. Microbiol.* **52**, 745–778
- Nussenzweig, R. S., and Nussenzweig, V. (1984) *Philos. Trans. R. Soc. Lond. Biol. Sci.* **307**, 117–128
- Rudd, P. M., Elliott, T., Cresswell, P., Wilson, I. A., and Dwek, R. A. (2001) *Science* **291**, 2370–2376
- Plebanski, M., Flanagan, K. L., Lee, E. A., Reece, W. H., Hart, K., Gelder, C., Gillespie, G., Pinder, M., and Hill, A. V. S. (1999) *Immunity* **10**, 651–660
- Millar, A. E., Wleklinski-Lee, M., and Kahn, S. J. (1999) *J. Immunol.* **162**, 6092–6099
- Gonçalves, M. F., Umezawa, E. S., Katzin, A. M., de Souza, W., Alves, M. J., Zingales, B., and Colli, W. (1991) *Exp. Parasitol.* **72**, 43–53
- Barros, H. C., Da Silva, S., Verbisek, N. V., Araguth, M. F., Tedesco, R. C., Procopio, D. O., and Mortara, R. A. (1996) *J. Eukaryot. Microbiol.* **43**, 275–285